Quantum Electronics **50** (7) 694–699 (2020)

CONTROL OF LASER RADIATION PARAMETERS https://doi.org/10.1070/QEL17193

Phasing of seven-channel fibre laser radiation with dynamic turbulent phase distortions using a stochastic parallel gradient algorithm at a bandwidth of 450 kHz

M.V. Volkov, S.G. Garanin, T.I. Kozlova, M.I. Konoval'tsov, A.V. Kopalkin, R.S. Lebedev, F.A. Starikov, O.L. Techko, S.V. Tyutin, S.V. Khokhlov, V.S. Tsykin

Abstract. **We have demonstrated an experimental setup for the coherent phasing of a seven-channel fibre laser system (λ = 1064 nm) in a scheme comprising a master oscillator and a set of parallel amplifiers with lithium niobate-based fibre-optic phase modulators. Using a stochastic parallel gradient algorithm, an instrumental phase modulator control unit ensures a bandwidth of the system up to 450 kHz. The effectiveness of phasing of light transmitted through a turbulent medium with a characteristic time scale τ_{turb} has been studied experimentally as a function of phasing time τ_{ph}. The results demonstrate that the average Strehl ratio begins to rise at $\tau_{turb}/\tau_{ph} \geqslant 2$ and that the effectiveness of compensation for dynamic phase distortions in the beam propagation path rises sharply at $\tau_{turb}/\tau_{ph} \approx 20$. For $\tau_{turb}/\tau_{ph} \geqslant 30-40$, the average Strehl ratio remains constant at the level reached.**

Keywords: *phasing of laser radiation, fibre laser, stochastic parallel gradient algorithm, atmospheric turbulence.*

1. Introduction

The radiant intensity of laser radiation is directly proportional to its power and inversely proportional to the square of its angular divergence, so it can be increased by raising the laser power and/or reducing the divergence of the laser beam. The laser power depends on the energy potential of the gain medium, and the beam divergence depends on the beam aperture size and optical inhomogeneities of the gain medium and channel. In the case of a single-channel laser, it is usually impossible to significantly raise its power with no increase in beam divergence or reduce the beam divergence with no power loss. Coherent phase combining of light from N parallel laser channels ensures both an increase in power and a decrease in beam divergence (see e. g. Refs [1–3]). As a result, the power of the system is N times that in the case of a single channel, and the radiant intensity can increase by N^2 times because of the decrease in divergence due to the increase in the total coherent aperture of the system. An important point is that the latter is only possible if the light in the channels at the output of the laser system has equal phases. Without phasing, the average radiant intensity of light scales linearly with N, like its power.

Researchers at the Institute of Laser Physics Research (ILPR), All-Russia Research Institute of Experimental Physics, Russian Federal Nuclear Center, studied the phasing of multichannel cw laser light (with diffraction-limited beam divergence in each channel) using a stochastic parallel gradient (SPG) algorithm [4]. The SPG algorithm is a two-step iterative procedure for optimising a particular criterion functional. In the first step, random small phase shifts are made in the channels. In the second, 'intellectual', step, correction is performed. Calculational optimisation made it possible to find conditions for raising the convergence rate of the SPG algorithm to two or three iterations per laser channel and experimentally demonstrate, in dynamics, SPG phasing of a laser beam divided into a number of channels, but at a relatively low speed [5]. In a later study [6], SPG phasing of a seven-channel fibre laser system [master oscillator (MO) and seven parallel amplifiers] was implemented experimentally, with compensation for its internal thermal phase distortions at a 14-kHz bandwidth of the system.

Phasing at the output of a multichannel laser system ensures compensation for phase inhomogeneities developing inside the system. Of particular interest is the phasing of a system over large distances in an optically inhomogeneous medium, e. g. in a turbulent atmosphere. Unlike phasing methods based on phase measurement (see e. g. Pyrkov et al. [7]), the SPG algorithm allows for the phasing of a multichannel beam through an optically inhomogeneous medium via optical control over focusing on a target in a feedback loop [8]. Naturally, phasing effectiveness is influenced by both the length and time scales of phase fluctuations in the medium. As shown using calculations [9] and experimentally [10], phasing through a turbulent atmosphere is highly effective if the atmospheric coherence length (Fried parameter [11]) is of the same order as or exceeds the transverse size of one laser channel (subaperture).

The objectives of this work were to experimentally study the effect of the time scale of phase fluctuations in a medium with dynamic optical inhomogeneities on the phasing of multichannel laser light and establish a criterion for phasing effectiveness as a function of the relationship between the phasing time and the characteristic time for a 'frozen state' of turbulent phase fluctuations. This research became possible after the drastic increase in the speed of the SPG phasing system at the ILPR, with an increase in its bandwidth to 450 kHz.

M.V. Volkov, S.G. Garanin, T.I. Kozlova, M.I. Konoval'tsov, A.V. Kopalkin, R.S. Lebedev, F.A. Starikov, O.L. Techko, S.V. Tyutin, S.V. Khokhlov, V.S. Tsykin Institute of Laser Physics Research, All-Russia Research Institute of Experimental Physics, Russian Federal Nuclear Center, prosp. Mira 37, 607188 Sarov, Nizhny Novgorod region, Russia; e-mail: oefimova@otd13.vniief.ru

Received 19 November 2019; revision received 15 January 2020
Kvantovaya Elektronika **50** (7) 694–699 (2020)
Translated by O.M. Tsarev.

2. Experimental

The basic schematic of the phasing of light from a seven-channel fibre laser system (Fig. 1) is similar to that considered previously [9]. A two-stage master oscillator (*1*) (wavelength λ = 1064 nm, spectral linewidth of 10 kHz) is composed of a single-frequency semiconductor laser diode (*2*) and a diode-pumped (*4*) Yb^{3+}-doped fibre preamplifier (*3*). The degree of polarisation of the light at the MO output is 0.98. To maintain the degree of polarisation of the light, all other elements of the laser system were made of polarisation-maintaining fibre.

The MO beam splitting system (*5*) consists of three coupler stages (one of the eight channels was not used). The splitting ratio of each coupler at λ = 1064 nm is 50/50. After the beam splitting system, the light in each channel is launched into fibre amplifiers (*6*). Each amplifier has its own thermal stabilisation system and is pumped by a separate laser diode. The total output power is about 2 W.

The amplified light was directed to electro-optical fibre phase modulators (*7*) based on $LiNbO_3$ crystals (in the case of relatively low laser output power, it was unimportant whether the modulators were located before or after the amplifiers). After the phase modulators, there were patch cords (*8*). Next, the seven-channel laser light arrived at seven hexagonally arranged lenses (*9*), secured in a metallic mount. The geometry of the arrangement of the 68-mm-diameter collimating lenses in a sufficiently dense packing is shown in Fig. 2. The overall output laser aperture was 220 mm. The lens assembly was placed so that the common focal plane of the lenses was located on the end faces of the patch cords. After collimation, the laser light in the form of seven plane-parallel beams arrived at a double lens system (Fig. 1, *10*) with an equivalent focal length of 100 m. In the focal plane of the double lens system (in the far field) was placed a 0.2-mm-diameter diaphragm (*11*). The light transmitted through the diaphragm was detected by a photodiode (*12*). Under these conditions, the photodiode recorded the power of the seven-channel light in an angle of 0.002 mrad at a diffraction peak width of 0.013 mrad for the overall aperture, i.e. essentially the axial radiant intensity of the overall radiation, which is the criterion functional of the SPG algorithm. Note that the convergence rate of the SPG algorithm is independent of the diaphragm size if it does not exceed the diffraction limit [12]. To visualise the process, part of the light reflected from a wedge (*13*) was directed to the array of a CCD camera (*14*), also located in the focal plane of the double lens system (*10*). Turbulent phase distortions in the propagating beam were produced by a heated air flow from a fan heater (*15*), which was delivered to the large-aperture part of the beam, between the lens assembly (*9*) and the focusing lens system (*10*). The position of the fan heater remained unchanged in all our experiments.

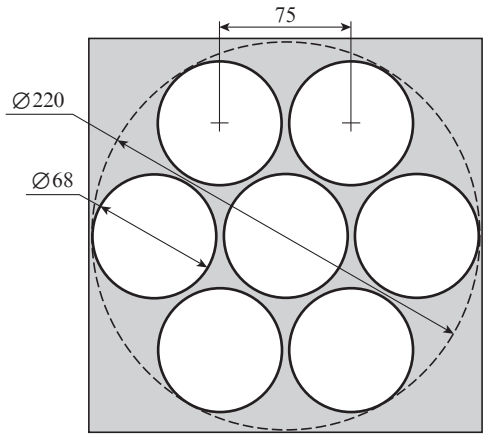

Figure 2. Geometry of the arrangement of the collimating lenses at the output of the system (the dimensions are given in millimetres).

With feedback in the phasing system turned on, the criterion functional (axial radiant intensity of radiation) detected by the photodiode (*12*) was fed to a control unit

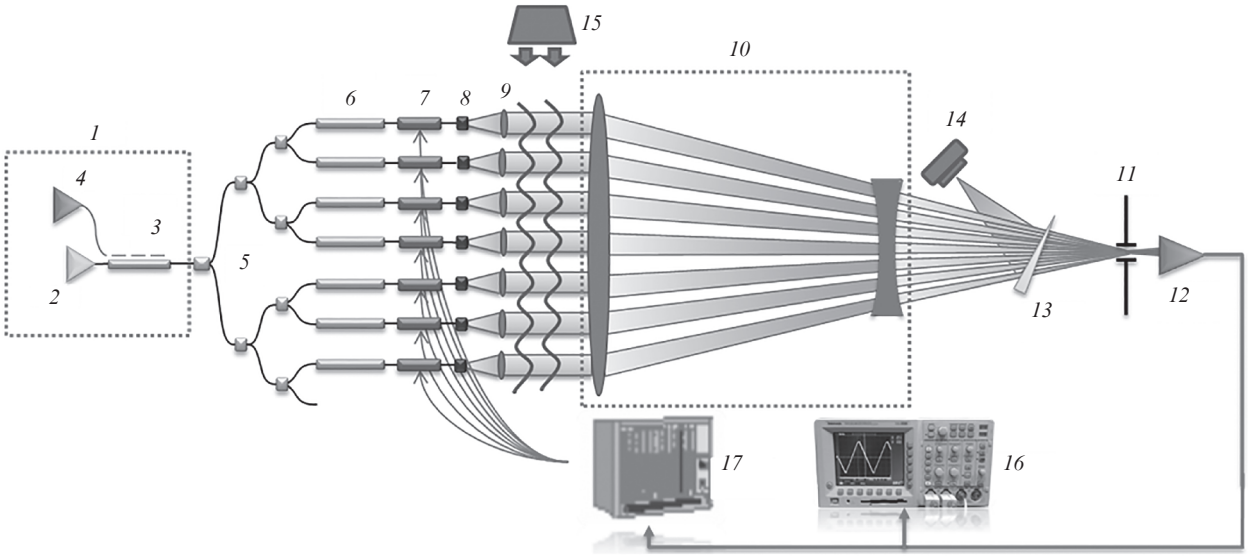

Figure 1. Basic schematic of the laser system: (*1*) master oscillator; (*2*) single-frequency laser diode; (*3*) preamplifier; (*4*) preamplifier pump diode; (*5*) beam splitting system; (*6*) amplifiers; (*7*) phase modulators; (*8*) patch cords; (*9*) lens assembly; (*10*) double lens system; (*11*) diaphragm; (*12*) photodiode; (*13*) wedge; (*14*) CCD camera; (*15*) fan heater; (*16*) oscilloscope; (*17*) phase modulator control unit.

(*17*), which generated voltages applied to the phase modulators (*7*) in accordance with the SPG algorithm. The electronic control unit is based on microcontrollers operating in parallel. In conjunction with the use of the high-speed phase modulators built in optical fibre, this solution allowed the bandwidth of the system to reach 450 kHz (the quantity inversely related to the closed cycle time, i.e. to the duration of one iteration step in the SPG algorithm). The exposure time of the photodiode is short compared to the closed cycle time.

In the first step of each iteration of the SPG algorithm, relatively small random test phase shifts with an amplitude $\pm\alpha$ are generated in parallel in the channels by the control unit with the help of the phase modulators. In the second iteration step, correction phase shifts with a preset amplitude are made in parallel in the channels. As a result, the criterion functional rises on average in comparison with the initial one. After that, the new value of the criterion functional is recorded and the next iteration is performed. As shown earlier [5], at a test phase shift amplitude $\alpha < 0.1\pi$ to each value of α there corresponds an optimal phase shift amplitude in the second step, which maximises the convergence rate of the SPG algorithm after a preset Strehl ratio is reached. For $\alpha \geqslant 0.1\pi$, the phasing process slows down with increasing α and becomes more unstable. For example, in the case of seven-channel laser radiation, for the Strehl ratio to reach 0.8 at $\alpha = 0.03\pi$ and 0.05π it is necessary to make on average 14 and 18 iterations (2 and 2.6 iterations per channel), respectively [5]. At $\alpha = 0.09\pi$, as many as 21 iterations (3 iterations per channel) are needed [6].

3. Experimental results

In an ideal case, a closed-cycle phasing system should ensure a diffraction-limited intensity distribution in the far field, independent of the phase mismatch in the channels and phase distortions in the beam path. To ensure the highest convergence rate of the SPG algorithm, its optimal parameters determined previously [5] were used in our experiments.

Figure 3 shows calculated and experimentally determined instantaneous far-field intensity distributions for a seven-channel fibre laser after completion of the phasing process and the corresponding intensity profiles along one of the axes. To minimise the effect of the finiteness of the bandwidth of the phasing system, there were no dynamic phase distortions in the scheme. In such a case, phase distortions are only determined by the optical path difference in the channels (Fig. 1) and the thermal phase noise in the amplifiers, which varies rather smoothly with time in the hertz range [13]. In the experiment under consideration, the phasing system operated at a bandwidth of 234 kHz and a test phase shift amplitude $\alpha = 0.03\pi$.

It is seen that the calculated and experimentally measured intensity ratios of the central and side maxima in the far field agree well. Therefore, without significant dynamic

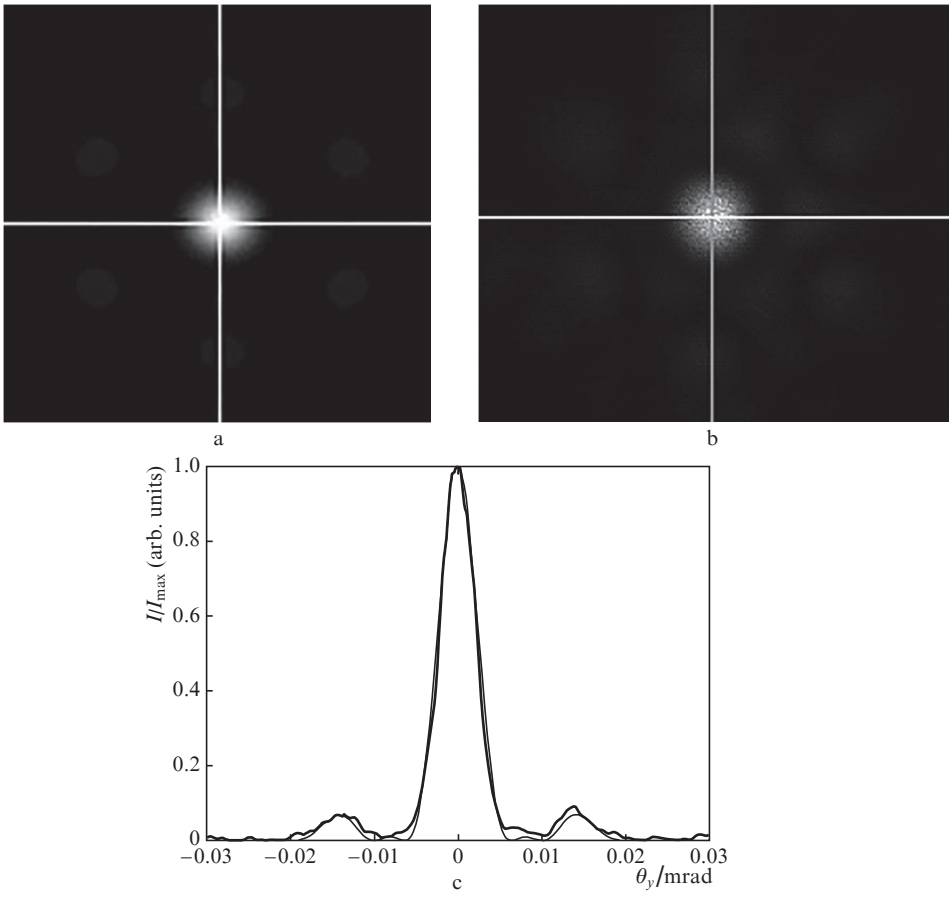

Figure 3. (a) Calculated and (b) experimentally determined far-field intensity distributions for seven phased channels of a fibre laser and (c) *y*-axis intensity profiles (the thick solid line represents the experimental data and the thin solid line represents the calculation results).

phase distortions in the beam path, the phasing system based on the SPG algorithm ensures a near diffraction-limited divergence of seven-channel laser radiation and a near unity Strehl ratio. Since the angular size of the diaphragm (*11*) in Fig. 1 is considerably smaller than the diffraction-limited one, the Strehl ratio in our experiment is a normalised signal from the photodiode, U/U_{max}, where U_{max} is the average signal with feedback on, without dynamic distortions in the beam path.

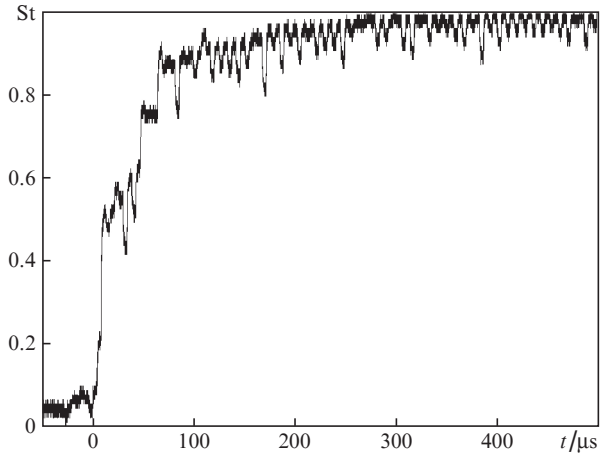

Figure 4. Time dependence of the experimentally determined Strehl ratio after turning on feedback.

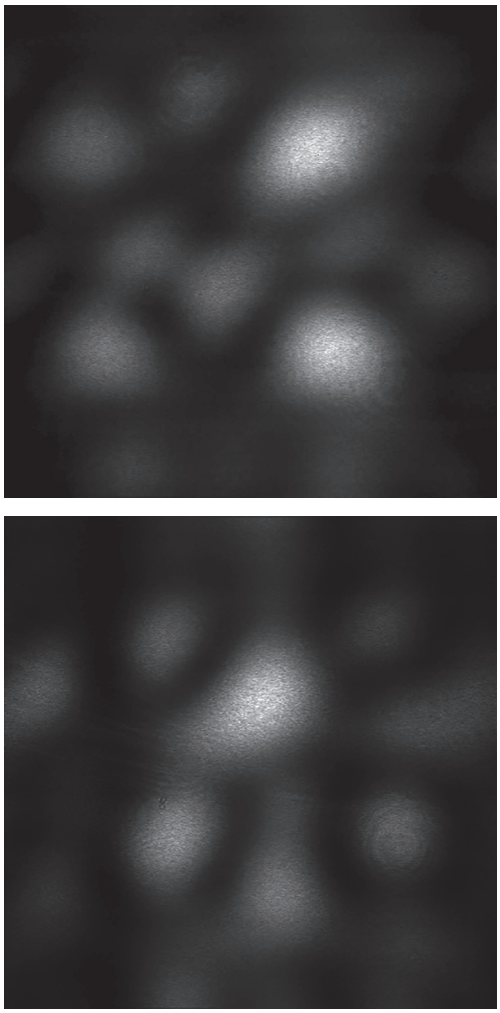

Figure 5. Instantaneous far-field intensity distributions for seven laser channels in the presence of dynamic phase distortions in the beam path.

Consider how the phasing process proceeded and what time was needed for the laser system to be phased, i. e. for the far-field intensity distribution to take the form shown in Fig. 3. Figure 4 shows a typical time dependence of the experimentally determined Strehl ratio St with feedback turned on at time $t = 0$. Previously reported calculation results and experimental data [5] indicate that, at a test phase shift amplitude $\alpha = 0.03\pi$ and optimal parameters of the SPG procedure, it is necessary to make on average two iterations per channel, i. e. 14 two-step iterations for a seven-channel laser beam, to reach St = 0.8. As seen in Fig. 4, turning on feedback increased the Strehl ratio from about 0.03 to 0.8–0.9 in 70–100 μs. At a 234-kHz bandwidth of the system, this corresponds to 8–12 two-step iterations of the SPG algorithm (i. e., in the experimental implementation in question, the required number of iterations is even smaller than its average). Thus, knowing the bandwidth of the system and the convergence rate of the SPG algorithm, we can estimate the average phasing time τ_{ph} as the product of the iteration time and the average number of iterations needed to reach St = 0.8. For example, under the experimental conditions of this study, the phasing time is $\tau_{ph} = (2/234\ \text{kHz}) \times 14 \approx 120\ \mu\text{s}$.

Consider now the phasing process in the presence of considerable dynamic refractive index fluctuations in the beam path. Turning on the fan heater (Fig. 1, *15*) produces dynamic optical inhomogeneities in the beam path and, as a consequence, the temporal spectrum of far-field oscillations of the axial radiant intensity (or the Strehl ratio) of the overall radiation acquires additional frequencies. Figure 5 presents examples of a characteristic instantaneous far-field multichannel beam intensity distribution in the presence of dynamic refractive index fluctuations.

Figures 6a and 6b illustrate the dynamics of the Strehl ratio of overall radiation and the frequency dependence of its spectral power in the presence of turbulent distortions in the beam path, with feedback off. The shape of the temporal spectrum of the Strehl ratio is characteristic of the refractive index spectrum of a turbulent medium and contains an inertial range where the spectral power falls off as a power law function. We are thus led to conclude that the inertial range of turbulence in our case lies between 1 and 10 Hz. At lower frequencies, the temporal spectrum plateaus, whereas at higher frequencies it falls off more rapidly. In the case of Kolmogorov turbulence, the spectral power of phase fluctuations in the inertial range follows a power law ($\sim \nu^{-5/3}$); in the case of coherent turbulence, there is a different exponent ($\nu^{-8/3}$) [14]. Kolmogorov (incoherent) turbulence results from a sequential decay of large random air eddies of various scales into smaller ones, but in our case the turbulence mechanism is determined by the decay of eddies having the same size, related to the fan blade size. The Strehl ratio is a space-integrated light parameter and, in the inertial range under consideration, its spectral power falls off as $\nu^{-8/3}$. In Fig. 6b, these data are represented by a dashed line.

Figure 6c shows the frequency dependence of spectral 'energy' – a frequency integral (normalised to unity) of the spectral power of the Strehl ratio. It is seen that the upper boundary of the inertial range coincides with the frequency within which essentially all spectral turbulence 'energy' lies.

Thus, it is reasonable to think that the characteristic time scale of phase distortions, τ_{turb}, produced by the air flow from the fan heater is 0.1 s.

Figure 7 illustrates the dynamics of the Strehl ratio at a bandwidth of 125 kHz and a test phase shift amplitude $\alpha = 0.03\pi$, with feedback on. It is seen that the Strehl ratio increased considerably (Fig. 6a).

Figure 8 shows the Strehl ratio averaged over 40 s with feedback on, in the presence of dynamic turbulent distortions, as a function of the ratio of the time scale of phase distortions, $\tau_{turb} = 0.1$ s, to the average phasing time τ_{ph} at test phase shift amplitudes $\alpha = 0.03\pi$, 0.05π and 0.09π. The data points corresponding to the largest τ_{turb}/τ_{ph} ratios, i.e. to minimum τ_{ph}, were obtained at the maximum bandwidth, 450 kHz. In our experiments, τ_{ph} was increased via a factitious reduction in the bandwidth of the system: an increase in the criterion functional measurement time in each iteration of the SPG algorithm (such a mechanism for reducing the bandwidth appears natural for a real situation in which the problem of weak signal is encountered). It is seen that, with feedback on, the average Strehl ratio begins to increase for $\tau_{turb}/\tau_{ph} > 2$, and the effectiveness of compensation for dynamic phase distortions rises sharply at $\tau_{turb}/\tau_{ph} \approx 20$, i.e. when the phase correction time is a factor of 20 shorter than the characteristic time for turbulent phase changes. For $\tau_{turb}/\tau_{ph} \geqslant 30-40$, the average Strehl ratio remains constant at the level reached (~ 0.7), having increased by about six times relative to a dephased state. The smaller Strehl ratio (~ 0.65) at a test phase shift amplitude $\alpha = 0.09\pi$ is due to the proximity of α to 0.1π. As shown earlier [5], this leads to a higher variance of criterion functional fluctuations in the case of SPG phasing. We have considered the $\alpha = 0.09\pi$ case to demonstrate what can be caused by a forced increase in α, which is necessary, e.g., at a high noise contamination level of a criterion functional.

The criteria found above are independent of the test phase shift amplitude α in the SPG algorithm, which influences only its convergence rate, and depend only on the τ_{turb}/τ_{ph} ratio. We are thus led to conclude that these criteria are independent of the algorithm used to control the phase of multichan-

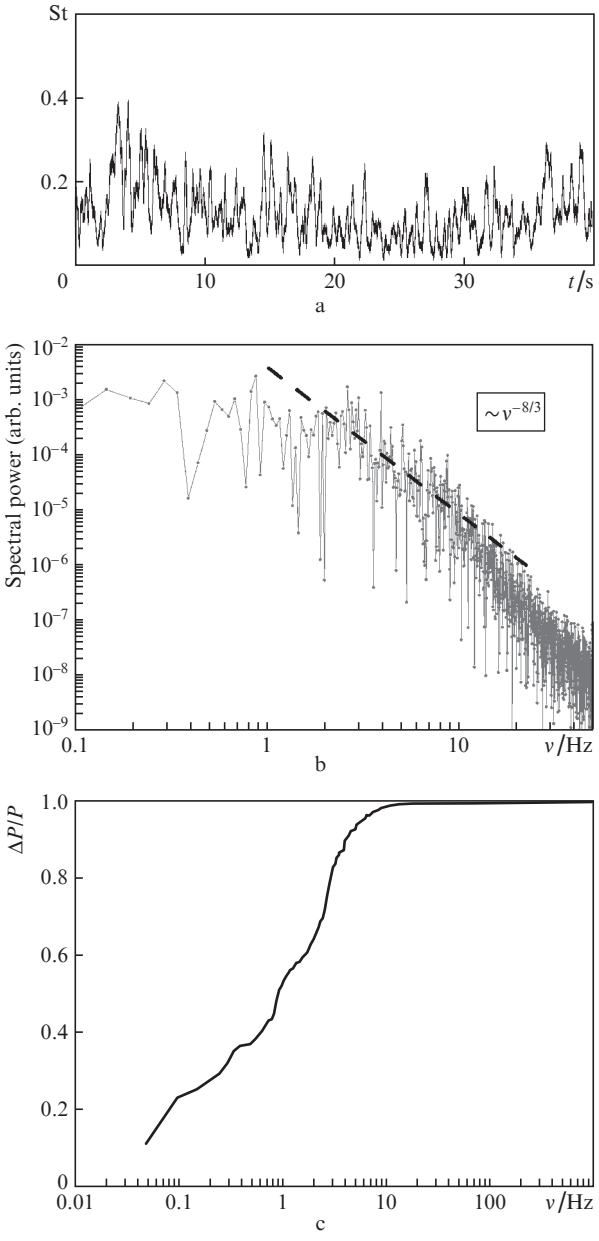

Figure 6. (a) Dynamics of the Strehl ratio, (b) its power spectrum with feedback off and (c) frequency dependence of the integral (normalised to unity) of the spectral power of the Strehl ratio.

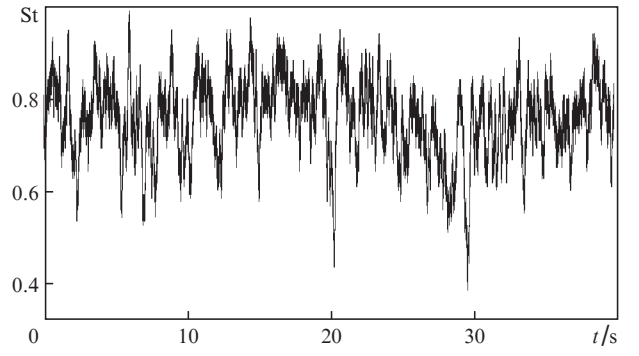

Figure 7. Dynamics of the Strehl ratio with feedback on.

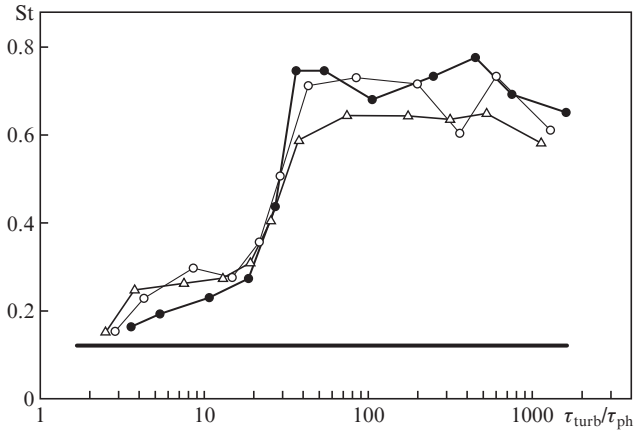

Figure 8. Average Strehl ratio as a function of the ratio of the characteristic time of phase distortions, τ_{turb}, to the average phasing time τ_{ph} at test phase shift amplitudes $\alpha = 0.03\pi$ (●), 0.05π (○) and 0.09π (△). The horizontal solid line represents the average Strehl ratio with feedback off.

nel laser radiation and the number of phased channels. Some details of St as a function of τ_{turb}/τ_{ph} are obviously dependent on the shape of the spectrum of dynamic phase distortions. In particular, as pointed out by Rukosuev et al. [15], in the case of adaptive compensation of harmonic oscillations the signal amplitude varies insignificantly even when the correction time is a factor of 10 shorter than the oscillation period.

The question that now arises is why does dynamic phasing increase the Strehl ratio from 0.12 to 0.7, and not to 1, i.e. by six times and not by the theoretically predicted $N = 7$ times, in contrast to the data in Figs 3 and 4? As shown earlier [9], the phasing of multichannel laser radiation through a turbulent atmosphere is highly effective if the atmospheric coherence length (Fried parameter) is larger than or of the order of the transverse size of one laser channel. Since the maximum Strehl ratio obtained in our experiments with dynamic phase distortions in the beam path is about 0.7, it is reasonable to assume that, according to previously reported results [9], the coherence length in these experiments is about half the transverse size of the laser channels. It is seen in Fig. 5, where the number of spots in the far field slightly exceeds the number of channels, and in Fig. 6a, where the average Strehl ratio of dephased light is less than $1/N = 1/7$.

4. Conclusions

We have produced an experimental setup for the coherent phasing of a seven-channel fibre laser system ($\lambda = 1064$ nm) in a scheme comprising a single-channel MO and a set of parallel amplifiers with lithium niobate-based fibre-optic phase modulators and an electronic instrumental modulator control unit. The phase modulators are controlled using a two-step iterative SPG algorithm. The modulator control unit is based on microcontrollers and ensures a bandwidth of the phasing system up to 450 kHz in a closed cycle.

The setup has been used to experimentally assess the effectiveness of phase combining of seven-channel laser system light transmitted through a medium with turbulent phase distortions having a characteristic time scale τ_{turb}, with the phasing time τ_{ph} varied. The results demonstrate that the average Strehl ratio begins to rise at $\tau_{turb}/\tau_{ph} \approx 2$ and that the effectiveness of compensation for dynamic phase distortions in the beam propagation path rises sharply at $\tau_{turb}/\tau_{ph} \approx 20$. For $\tau_{turb}/\tau_{ph} \geqslant 30-40$, the average Strehl ratio remains constant at the level reached, which is high if the atmospheric coherence length (Fried length) is of the order of (or exceeds) the aperture size of one channel in the system.

References

1. Fan T.Y. *IEEE J. Sel. Top. Quantum Electron*, **11**, 567 (2005).
2. Brignon A. (Ed). *Coherent Laser Beam Combining* (Berlin: Wiley, 2013).
3. Protz R., Zoz J., Geidek F., Dietrich S., Fall M. *Proc. SPIE*, **8547**, 854708-1 (2013).
4. Garanin S.G., Manachinsky A.N., Starikov F.A., Khokhlov S.V. *Optoelectron. Instrum. Data Process.*, **48** (2), 134 (2012) [*Avtometriya*, **48** (2), 30 (2012)].
5. Volkov V.A., Volkov M.V., Garanin S.G., Dolgopolov Yu.V., Kopalkin A.V., Kulikov S.M., Starikov F.A., Sukharev S.A., Tyutin S.V., Khokhlov S.V., Cheparin D.A. *Quantum Electron.*, **43** (9), 852 (2013) [*Kvantovaya Elektron.*, **43** (9), 852 (2013)].
6. Volkov M.V., Garanin S.G., Dolgopolov Yu.V., Kopalkin A.V., Kulikov S.M., Sinyavin D.N., Starikov F.A., Sukharev S.A., Tyutin S.V., Khokhlov S.V., Cheparin D.A. *Quantum Electron.*, **44** (11), 1039 (2014) [*Kvantovaya Elektron.*, **44** (11), 1039 (2014)].
7. Pyrkov Yu.N., Trikshev A.I., Tsvetkov V.B. *Quantum Electron.*, **42** (9), 790 (2012) [*Kvantovaya Elektron.*, **42** (9), 790 (2012)].
8. Weyrauch T., Vorontsov M.A., Carhart G.W., Beresnev L.A., Rostov A.P., Polnau E.E., Liu J.J. *Opt. Lett.*, **36** (22), 4455 (2011).
9. Volkov V.A., Volkov M.V., Garanin S.G., Starikov F.A. *Quantum Electron.*, **45** (12), 1125 (2015) [*Kvantovaya Elektron.*, **45** (12), 1125 (2015)].
10. Weyrauch T., Vorontsov M., Mangano J., Ovchinnokov V., Bricker D., Polnau E., Rostov A. *Opt. Lett.*, **41** (4), 840 (2016).
11. Fried D.L. *J. Opt. Soc. Am.*, **56** (10), 1380 (1966).
12. Volkov V.A., Volkov M.V., Garanin S.G., Dolgopolov Yu.V., Kopalkin A.V., Kulikov S.M., Starikov F.A., Sukharev S.A., Tyutin S.V., Khokhlov S.V. *Tr. RFYaTs VNIIEF*, **19**, 404 (2014).
13. Augst S.J., Fan T.Y., Sanchez A. *Opt. Lett.*, **29** (5), 474 (2004).
14. Nosov V.V., Lukin V.P., Nosov E.V., Torgaev A.V. *Opt. Atmos. Okeana*, **32** (3), 228 (2019).
15. Rukosuev A.L., Kudryashov A.V., Lylova A.N., Samarkin V.V. *Opt. Atmos. Okeana*, **28** (2), 189 (2015).